Desalination and Water Treatment
www.deswater.com

doi: 10.5004/dwt.2019.23120

137 (2019) 76–87
January

Application of several plant roots as biosorbent and nanobiosorbent for the removal of Pb^{2+} and Zn^{2+} from aqueous solutions

Hassan Karami[a,*], Tooran Mohammadi[b]

[a]*Department of Chemistry, Payame Noor University, PO Box 19395-3697, Tehran, Iran, email: karami_h@yahoo.com*
[b]*Department of Chemistry, Nano Research Laboratory, Payame Noor University, Abhar, Iran, email: t.maohamadi93@gmail.com*

Received 18 November 2017; Accepted 13 September 2018

ABSTRACT

The aim of this paper is full study about the abilities of the roots of castor, pear, peach, apple, almond, walnut, sour cherry, berry, ginger, sunflower, red flower, mallow, grapevine, hot pepper, hollyhock, tomato, astragalus, and black eggplant as biosorbents for the removal of heavy metal ions from water. The obtained results indicate that the grapevine root particles can adsorb heavy metal ions better that other roots and also, lead and zinc ions can be better adsorbed than other ions. In the next step, the grapevine root is milled into nanoparticles by an innovative ball mill. The prepared nanoparticles are characterized by DLS, transmission electron microscopy, scanning electron microscopy, and Fourier-transform infrared spectroscopy. The results show that the average diameter of grapevine root nanoparticles (GRN) is 63 nm. The prepared GRN is used as nanobiosorbent to remove lead and zinc ions from water. Based on the experimental results, Pb^{2+} and Zn^{2+} ions can quantitatively remove from water by a spontaneous exothermic process in the conditions including pH 4, initial solution volume 50 mL, initial concentration of each metal ion 50 mg L^{-1}, sorbent dosage 4 g L^{-1}, and contact time 30 min at room temperature. The isothermal and kinetic studies show that the adsorption of Pb^{2+} and Zn^{2+} ions on GRN can be well described by Langmuir isotherm and pseudo-second-order kinetic models. Based on the Langmuir isotherm model, the maximum capacities are found 24.6 and 26.3 mg g^{-1} for the adsorption of Pb^{2+} and Zn^{2+} ions on GRN, respectively.

Keywords: Grapevine root; Biosorbent; Nanosorbent; Heavy metal; Ion removal

1. Introduction

The entry of heavy metal ions into the water and soil can lead to serious environmental hazards, even at trace amounts [1]. The hazardous metal ions such as Pb, Zn, Cd, Hg, and As can enter into the environment from different sources such as batteries, metal plating, and mineral processing [2]. The heavy metal ions are not degradable into harmless products [3]. Lead and zinc are widely used in various industries, can discharge into the wastewater and causes many harmful effects to human health [4,5]. The allowable concentrations of Pb^{2+} and Zn^{2+} have been determined 0.05 and 4 mg L^{-1}, respectively, by World Health Organization (WHO) [6,7].

The chemical precipitation, membrane and electrochemical separations, and ion exchange were introduced for the removal of toxic heavy metal ions [8,9]. The most of the above-mentioned methods have some limitations such as difficult operation, high cost, unusable on large scale, and low efficiencies at higher concentrations of metal ions. Adsorption as one of the most efficient removal methods is generally recommended due to lower environmental impacts, low cost, treatment stability, and easy operation. Many chemical and natural adsorbents have been introduced for the removal of Zn^{2+} and Pb^{2+} ions from water [10,11].

Recently, various nanosorbents have been used to remove heavy metal ions from water and wastewater because of their large specific surface areas [12–14]. Recently, biosorbents have been widely used for the removal of toxic compounds from water [15–19].

* Corresponding author.

The plant root is usually underground portion of a plant that lacks buds, leaves, or nodes and serves as support, draws minerals and water from the surrounding soil, and sometimes stores food. Major uptake of water and other minerals by plant is done in plant root. Therefore, it seems that roots of plants to be suitable biosorbent for the removal of metal ions from water. For the first time as a full study, 18 different plants roots including castor, pear, peach, apple, almond, walnut, sour cherry, berry, ginger, sunflower, red flower, mallow, grapevine, hot pepper, hollyhock, tomato, astragalus, and black eggplant were examined as adsorbents for the removal of some heavy metal ions from water. Finally, grapevine roots particles (GRP) and grapevine root nanoparticles (GRN) have been produced and extensively investigated as a suitable adsorbent for the removal of lead and zinc ions from water because of their simplicities, high efficiencies, and high adsorption capacities.

2. Experimental

2.1. Materials

$Fe(NO_3)_2$, $Pb(NO_3)_2.H_2O$, $Zn(NO_3)_2.6H_2O$, $CuSO_4.5H_2O$, $Mn(NO_3)_2.4H_2O$, $NaNO_3$, $MgSO_4$, and HNO_3 as the chemicals in analytical grade were purchased from Merck and used without further purification. Double-distilled water was used in all experiments. The roots of some plants (castor, pear, peach, apple, almond, walnut, sour cherry, berry, ginger, sunflower, red flower, mallow, grapevine, hot pepper, hollyhock, tomato, astragalus, and black eggplant) were collected from Abhar city (Zanjan, Iran).

2.2. Instrumentals

The prepared GRN was characterized by scanning electron microscopy (SEM; Vp 1455) and transmission electron microscopy (TEM; Zeiss EM10C). Fourier-transform infrared spectroscopy (FT-IR; Thermo Scientific Nicolet IS 10) was used to study the mechanism of lead and zinc ions adsorption on GRN. Size distribution diagram of the samples was obtained by DLS (Malvern Instruments Ltd, Zeta Sizer Ver. 6.32). Flame atomic absorption spectrophotometer (GBC, Sense AA, Australia) was used to demine the residual concentrations of the heavy metal ions. A 2,500 rpm centrifuge (Wagtech Co. C257-176) and also cellulose acetate membrane (0.45 μm, Micropore) were used to separate the GRN from solution in adsorption and desorption studies, respectively.

2.3. Experimental procedures

2.3.1. Production of micrometer and nanometer sized-root particles

The plant roots are collected. After separation of any non-objective particles, the roots of each plant were washed and dried under sunlight for 1 week. For production of micrometer-sized powder, 10 g from each plant root was crushed by porcelain mortar to obtain uniform powder. The prepared powders were graded using 500 and 625 mesh laboratory sieves. The particle size of the graded powders was estimated by using Tyler standards of sieves 20–25 μm.

For production of grapevine nanopowder, grapevine root was mill by an innovative ball mill which was explained in [20]. For this propose, 100 g of each plant root was milled in ball mill with a specified formulation of steel balls according to Table 1. Sampling of powder was done at 20 min, 2, 4, 6, and 8 h ball milling.

2.3.2. Adsorption experiments

First, adsorption batch studies were performed with the prepared micrometer-sized root particles (MSRP). In this step, 200 mg MSRP of each plant was added to 50 mL of each metal ion (Pb^{2+}, Cu^{2+}, Zn^{2+}, Fe^{2+}, Mn^{2+}, and Mg^{2+}) solution with initial concentration of 50 ppm with pH 4. The mixtures were stirred for 30 min at 400 rpm and then, MSRP was separated from the solution by centrifuging. The residual concentrations of the proposed ions were determined by the flame atomic absorption spectroscopy. In the next steps, the experimental conditions for the removal of lead and zinc ions were fully studied. The effect of pH was investigated at 25°C and initial concentration 50 mg L^{-1}. pH adjustments were done by using 0.1 M HNO3 solution and 0.1 M NaOH. In adsorption experiments, the removal efficiency was calculated by the following equation:

$$\text{Efficiency}\left(\%\right)=\frac{C_i-C_f}{C_i}\times 100 \tag{1}$$

where C_i (mg L^{-1}) and C_f (mg L^{-1}) are ion concentrations before and after mixing with sorbent, respectively. The equilibrium adsorption capacity, q_e (mg g^{-1}) was calculated using the mass balance equation (Eq. (2)):

$$q_e=\frac{\left(C_i-C_e\right)}{m}\times V \tag{2}$$

where C_e (mg L^{-1}) is the equilibrium concentration of metal ions. V (mL) is the sample volume and m (mg) is the amount of sorbent.

3. Results and discussion

3.1. Characterization of grapevine root nanoparticles

All micrometer-sized samples were graded by using two laboratory sieves therefore, they were used without any further characterization. The GRN were produced by using the innovative vibrational ball mill. The ball milling process

Table 1
The specified formulation of balls used in the innovative ball mill

Diameter (mm)	Number
5	50
10	30
15	20
20	10
24	5

was done in 20 min, 2, 4, 6, and 8 h. The prepared samples in different ball milling times were characterized by DLS. The summary of DLS results is shown in Fig. 1. As can be seen in Fig. 1, the average particles sizes of the GRN are decreased from 2,000 to 60 nm when the ball milling time is increased from 20 min to 6 h. The difference between the average particles sizes of two samples was produced at 6 and 8 h ball milling are not significant therefore, the suitable ball milling time for the production of GRN is 6 h.

As an example, the characterization results of the produced GRN in 6 h were shown in Fig. 2.The SEM image in Fig. 2(a) shows that the GRN was strongly agglomerated. The sample was fully dispersed in ethanol by ultrasonic irradiation. During ultrasonic irradiation, the agglomerated particles are separated from each other. The solvent of the mixture was evaporated and the residual paste was dried and crushed. The final nanopowder was analyzed by TEM. As it can be seen in TEM micrograph (Fig. 2(b)), the sample consists uniform nanoparticles with average diameter of 30 nm. Based on the DLS diagram (Fig. 2(c)), the sample consists nanoparticles in the range of 45–90 nm with average particle size of 63 nm. The difference between TEM and DLS results is due to the agglomeration of nanoparticles. The result of TEM is more reliable than that of DLS.

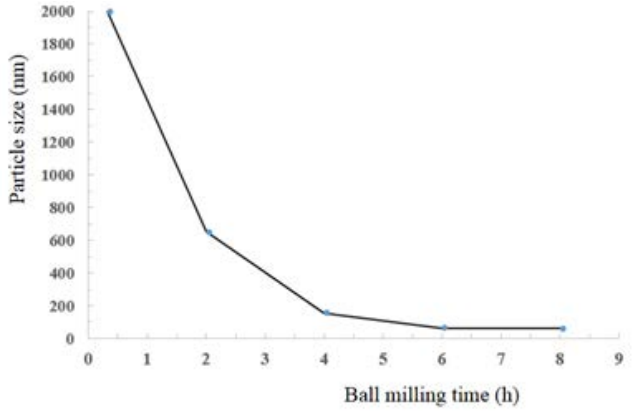

Fig. 1. Effect of ball milling time on the average particle size of GRN.

3.2. Application of plants roots as biosorbent

3.2.1. Biosorption of different metal ions

The efficiencies of 18 kinds of plants roots as biosorbent in same experimental conditions including 50 mL initial solution, pH 4, 50 mg L^{-1} initial concentration of each metal ion, contact time 30 min, and 4 g L^{-1} sorbent dosage at room temperature were separately examined for Mg^{2+}, Zn^{2+}, Cu^{2+}, Pb^{2+}, Fe^{2+}, and Mn^{2+} ions. Table 2 shows the removal efficiencies of some heavy metal ions by different plant roots. Based on Table 2, the following results can be obtained:

- The roots particles of pear, sour cherry, sunflower, mallow, grapevine, hot pepper, hollyhock, tomato,

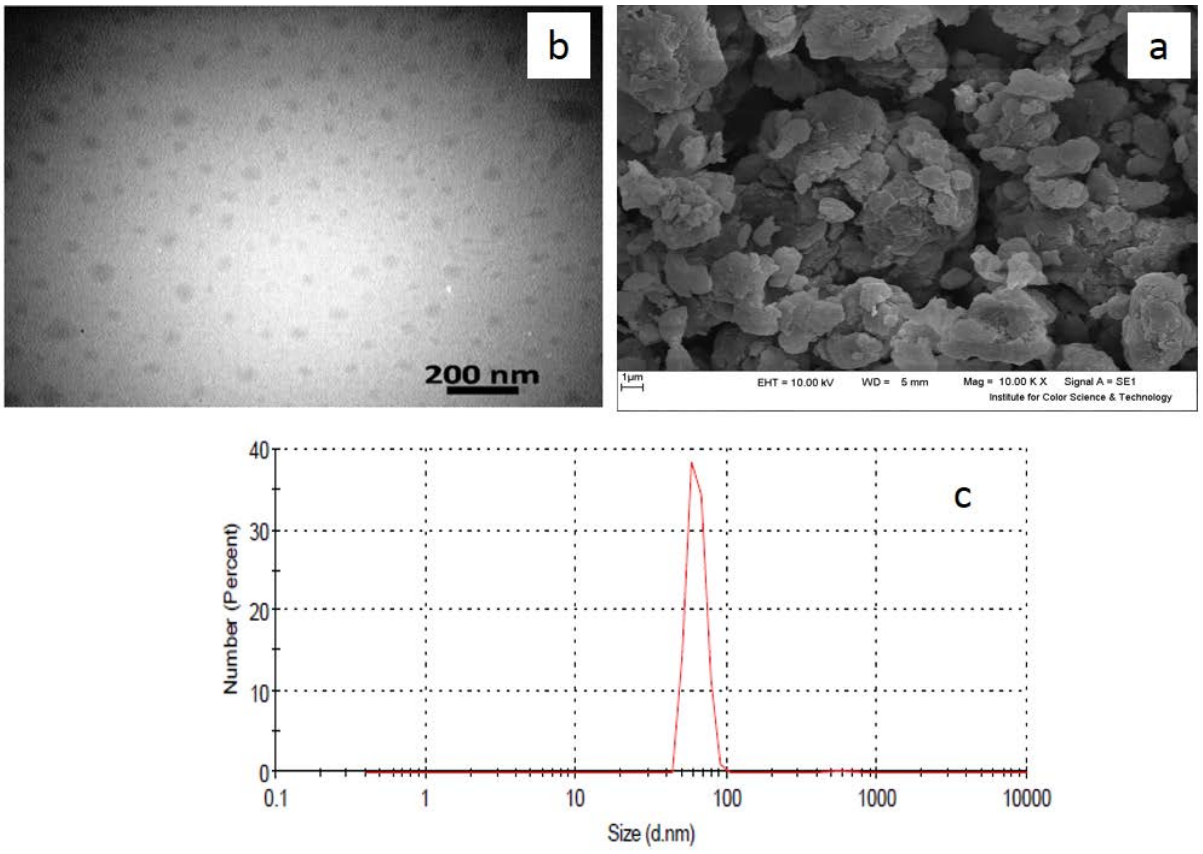

Fig. 2. SEM image (a), TEM micrograph (b), and DLS size distribution diagram (c) of the prepared GRN within 6 h ball milling.

astragalus, and eggplant can be used as efficient biosorbents (removal efficiency more than 90%) for the removal of lead ions (marked in bold in Table 2).
- The roots particles of grapevine and eggplant can be used as efficient biosorbents (removal efficiency more than 90%) for the removal of lead and zinc ions (marked in bold italic in Table 2).
- All experiments in Table 2 were repeated two times. The relative standard deviation (RSD%) was calculated. The calculated RSD% was in the range 1.3%–2.1%. The results show that the presented method has acceptable accuracy.

A number of previous reports have illustrated the sorption potential of low-cost biomaterials for different metal ions [21–33]. The performance of different biosorbents is mainly based on the affinity of available functional groups to metal ions; for their removal/recovery from different solutions. In the work, all plant roots in Table 2 were studied by FT-IR (the results were not included in the paper). All spectrums show the presence of OH, NH, carbonyl (CO), and ester (CO) functional groups. The presence of the mentioned functional groups in biomass and their affinity for metal ions in sorption process has previously reported [34–38]. The neighboring groups of the mentioned donating groups in the plant roots are different. Therefore, donating groups (OH, NH, carbonyl CO, and ester CO) in the mentioned plants in Table 2 have different basic characters. Therefore, we suggest a scheme shown in Fig. 3 as an adsorption mechanism for the removal of heavy metal ions by plants roots. In interaction between root and metal ion, one to four chemical bands can be formed. Based on type of root, the strength of the formed bands will be different therefore, the removal efficiencies of heavy metal ions by the mentioned plants roots can be different. Based on the results (Table 2), the interaction between plant roots and Zn^{2+} and Pb^{2+} is stronger than other ions. It can be related to the best interaction between soft acid-soft bases.

Table 2
Removal efficiencies (%) of metal ions by some different micrometer-sized root particles

No.	Root name	Pb^{2+}	Zn^{2+}	Cu^{2+}	Fe^{2+}	Mn^{2+}	Mg^{2+}
1	Castor	75.7*	84.2	76.6	9.2	31.6	14.8
2	Pear	95.4	45.8	44.2	5.8	36.4	2.8
3	Peach	75.5	65.5	60.2	6.2	30.2	2.0
4	Apple	88.6	72.8	27.4	1.0	29.0	5.2
5	Almond	88.5	59.0	36.2	18.4	18.6	21.4
6	Walnut	87.7	99.1	44.7	3.2	30.2	37.6
7	Sour cherry	91.9	34.2	56.6	16.9	46.6	55.5
8	Berry	85.8	37.8	50.0	18.4	45.0	49.1
9	Ginger	78.2	81.0	52.8	60.4	13.4	10.6
10	Sunflower	95.5	65.1	75.8	1.4	24.5	6.4
11	Red flower	71.9	59.6	75.4	11.0	42.6	16.6
12	Mallow	100.0	55.1	40.2	24.4	39.4	13.0
13	*Grapevine*	94.6	98.7	43.4	20.4	30.3	44.5
14	Hot pepper	99.3	69.0	41.2	59.2	24.8	30.4
15	Hollyhock	93.5	35.6	72.6	25.6	58.8	9.6
16	Tomato	100.0	75.5	37.9	97.6	46.8	7.6
17	Astragalus	98.8	65.9	91.6	15.2	37.4	37.6
18	Eggplant	99.4	92.5	58.5	88.2	28.2	5.2

In all of these experiments, 100 mg biosorbent was added to 50 mL solution with pH containing metal ion with concentration of 50 mg L^{-1} and mixed for time 30 min at room temperature. All experiments were replicated two times
*All efficiencies are in percentage (%).

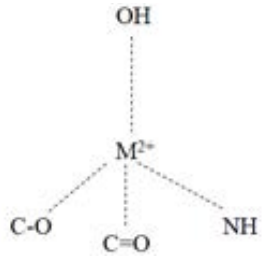

Fig. 3. The suggested interaction between metal ions and root particles. In each plant root, one of the four interactions is stronger.

3.2.2. The effect of pH on the removal of $Zn^{2+}$and Pb^{2+} by plant roots

The adsorption of heavy metal ions depends strongly on pH, and so the pH of the aqueous solution is an important controlling parameter in the adsorption process [39]. The influence of initial pH on adsorption percentage was studied in the range of 3–6 for the removal of Pb^{2+} and Zn^{2+} ions on 18 plant roots (Table 3). As Table 3 shows solution pH can strongly change the removal efficiency of lead ion as well as zinc ion. There are many hydroxyl groups on the surface of the plant root particles which deprotonate and converted to anionic groups and can adsorb metal ions (with positive charge) at pH higher than 3. On the other hand, lead and zinc ions can be treated with the hydroxide ions in the solution at pH higher than 5. Therefore, the maximum adsorption of lead and zinc ions takes place at pH about 4. At pH lower than 4, adsorption of metal ions is less, because the proton concentration is higher than those of metal ions so can compete with metal ions in adsorption on the root particles.

The presented data in Table 3 shows that the both grapevine and eggplant roots act as suitable sorbents for the removal of both Pb^{2+} and Zn^{2+} ions. However, due to the abundance of the root of the grapevine, especially in the studied area (Abhar), GRP was selected for further studies.

3.3. GRP or GRN?

GRP and GRN were used as biosorbent for the removal of lead and zinc ions in the same conditions (sample volume 50 mL, sorbent dosage 2 g L^{-1}, contact time 30 min, and temperature 25°C) in eight different concentrations of Zn^{2+} and Pb^{2+}. Fig. 4 shows the results these studies. Based on the presented data in Fig. 4, adsorption capacities of both Zn^{2+} and Pb^{2+} on GRN are 40% more than those of GRP. Therefore, GRN was selected for further studies.

Table 3
Removal efficiencies of metal ions by some different micrometer-sized root particles at different pHs

No.	Root Name	pH = 3		pH = 4		pH = 5		pH = 6	
		Pb^{2+}	Zn^{2+}	Pb^{2+}	Zn^{2+}	Pb^{2+}	Zn^{2+}	Pb^{2+}	Zn^{2+}
1	Castor	70.1*	19.0	75.7	84.2	87.2	50.9	73.9	37.0
2	Pear	91.1	20.5	95.4	45.8	100.0	42.5	90.9	44.8
3	Peach	72.1	60.2	75.5	65.5	85.1	63.0	85.1	59.8
4	Apple	84.8	23.5	88.6	72.8	98.0	67.8	92.5	31.0
5	Almonds	81.5	24.1	88.5	59.0	91.6	50.8	88.0	42.4
6	Walnut	86.8	91.4	87.7	99.1	93.2	54	89.7	39.3
7	Sour cherry	85.8	31.0	91.9	34.2	91.4	30.5	90.6	38.0
8	Berry	80.0	33.9	85.8	37.8	92.8	72.9	92.1	11.5
9	Ginger	86.7	18.5	78.2	81.0	94.8	60.1	93.5	45.5
10	Sunflower	92.4	49.5	95.5	65.1	85.9	53.8	80.6	59.2
11	Red flower	70.0	52.7	71.9	59.6	86.6	58.7	82.1	51.7
12	Mallow	85.2	52.1	100.0	55.1	98.7	55.3	87.6	38.0
13	**Grapevine**	88.8	51.2	**94.6**	**98.7**	98.4	71.8	90.3	56.0
14	Hot pepper	90.1	57.1	99.3	69.0	94.3	51.8	93.7	46.6
15	Hollyhock	89.5	25.0	93.5	35.6	100.0	41.5	93.8	41.0
16	Tomato	85.8	35.5	100.0	75.5	100.0	70.9	89.4	62.0
17	Astragalus	91.1	45.3	98.8	65.9	100.0	63.3	97.1	62.0
18	**Eggplant**	91.0	26.0	**99.4**	**92.5**	88.1	66.2	90.3	65.8

In all of these experiments, 100 mg biosorbent was added to 50 mL solution containing 50 mg L^{-1} metal ion (Zn^{2+} or Pb^{2+}) and mixed for 30 min at room temperature.
*All removal efficiencies are in percentage (%).

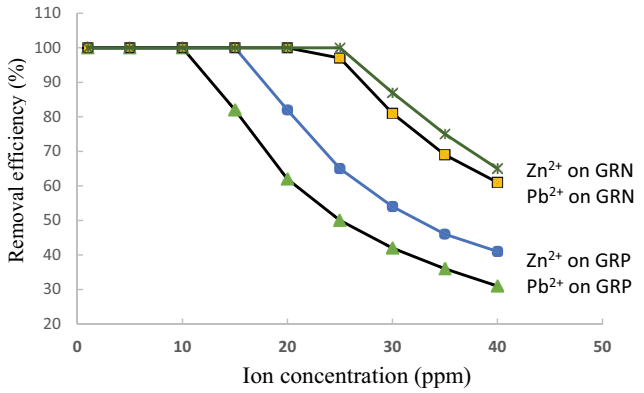

Fig. 4. Effect of ion concentration on the removal efficiency. In all of these experiments, 100 mg GRP or GRN was added to 50 mL solution with pH 4 containing 50 mg L^{-1} metal ion (Zn^{2+} or Pb^{2+}) and mixed for 30 min at room temperature.

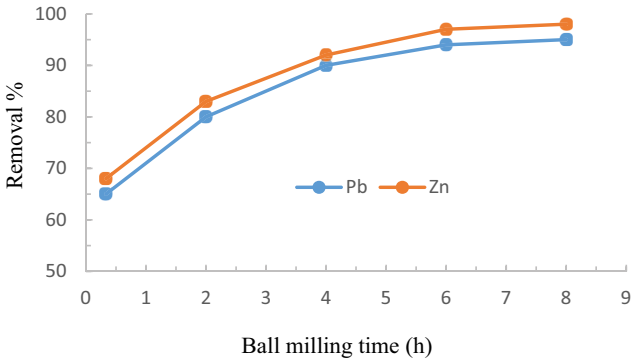

Fig. 5. The effect of ball milling time on lead ion removal efficiency. In all of these experiments, 100 mg GRN was added to 50 mL solution with pH 4 containing 50 mg L^{-1} metal ion (Zn^{2+} or Pb^{2+}) and mixed for 30 min at room temperature.

3.4. Adsorption studies on GRN

3.4.1. Effect of ball milling time on the removal efficiency of lead and zinc ions

The samples prepared at different ball milling times according to Fig. 1 were used as biosorbents for the removal of lead ions (Fig. 5). Fig. 5 shows that the ball milling time can obviously change the adsorption efficiency. The adsorption efficiencies of lead ions as well as zinc ions on GRN increase when the ball milling time increases. As it has been explained for the results of Fig. 1, the particles sizes of GRN samples decrease when the ball milling time increases. Therefore, these results show that smaller particles of adsorbent have bigger adsorption abilities. The results can be related to this fact that the smaller particles have a higher surface area/volume ratio.

3.4.2. Effect of pH

The influence of initial solution pH on adsorption efficiency was studied in the pH range of 3–6 for Pb^{2+} and Zn^{2+}

(Fig. 6). Fig. 6 shows that adsorption of Zn^{2+} ion is very sensitive to pH. At pH lower than 4, adsorption of zinc ions is less, because the proton concentration is higher than those of metal ions and such a situation was not favorable for the removal of zinc ions. Therefore, some of the negative sites of GRN will be occupied by proton ions so that the metal ions adsorption will be decreased. At pH higher than 4, adsorption of zinc ions is decreased due to the formation of $Zn(OH)^+$ ions [40].

pH dependency of lead ions is low in the pH range of 3–6. This fact due to the strong interaction between Pb^{2+} and functional groups of GRN. To confirm this fact, the effect of GRN on pH solution was investigated (Fig. 7).

In these experiments, the pH of each solution was determined before (pH_i) and after (pH_f) addition GRN ($\Delta pH = pH_f - pH_i$). Fig. 6 shows that the surface of GRN has no charge at pH 3.5. At pH lower and higher than 3.5, the surface of GRN has positive and negative charge, respectively. Therefore, pH 4 is suitable for the simultaneous removal of Zn^{2+} and Pb^{2+} ions.

3.4.3. Time dependency of metal ions adsorption on GRN and kinetics studies

To investigate the effect of contact time on the adsorption efficiency of lead ions on GRN, the removal values of lead ions by GRN are determined in different contact times (5–30 min). Fig. 8 shows the effect of contact time on the removal efficiencies of zinc and lead ions by GRN. As it can be seen in Fig. 8, the removal efficiency is increased when the contact time is increased. The metal ion removal is completed at 30 min. The required time for the quantitative sorption of each ion depends on the sorption kinetics.

In order to examine the diffusion mechanism of the adsorption process, two kinetic models were tested. The adsorption data were first fitted to pseudo-first-order kinetic model, which is given by Eq. (3) [41]:

$$\ln\left(q_e - q_t\right) = \ln q_e - k_1 t \tag{3}$$

where q_e and q_t are the amounts of adsorbed ion on sorbent (mg g^{-1}) at equilibrium and at contact time t (min), respectively, and k_1 is the pseudo-first-order rate constant (min^{-1}). The first-order-rate constant k_1 can be obtained from the slope of the plot In (q_e–q_t) versus t. Based on the obtained results, the R^2 values obtained are relatively small and the experimental q_e values do not agree with the values calculated from the linear plots. The results of these experiments were summarized in Table 4. In the next step, the data were examined by the pseudo-second-order kinetic model is given by Eq. (4) [42]:

$$\frac{t}{q_t} = \frac{1}{k_2 q_e^2} + \frac{t}{q_e} \tag{4}$$

where k_2 is the rate constant of pseudo-second-order adsorption (g mg^{-1} min^{-1}). Based on the experimental data of q, and t, the equilibrium sorption capacity (q_e), and the pseudo-second-order rate constant (k_2) can be determined from the slope and intercept of a plot of t/q versus t. It was found that the pseudo-second-order model gives a satisfactory fit to all of the experimental data. The parameters of the both pseudo-first-order and pseudo-second-order kinetics models are calculated and summarized in Table 4.

As Table 4 shows the both adsorption data of lead and zinc ions on GRN are fitted with pseudo-second-order kinetics model. The obtained results can be indicative of chemical

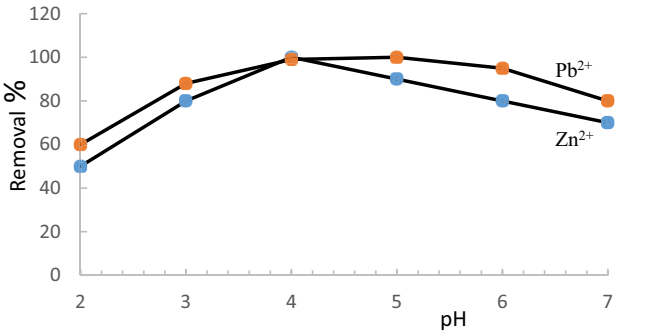

Fig. 6. Effect of solution pH on the removal efficiencies of lead and zinc ions. In all of these experiments, 100 mg GRN was added to 50 mL solution containing 50 mg L^{-1} metal ion (Zn^{2+} or Pb^{2+}) and mixed for 30 min at room temperature.

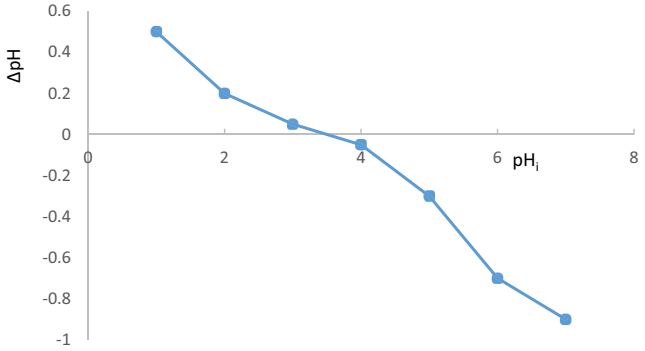

Fig. 7. Effect of GRN on solution pH at room temperature. At each pH, 100 mg GRN was added to 50 mL solution, mixed for 30 min, and the final pH was recorded.

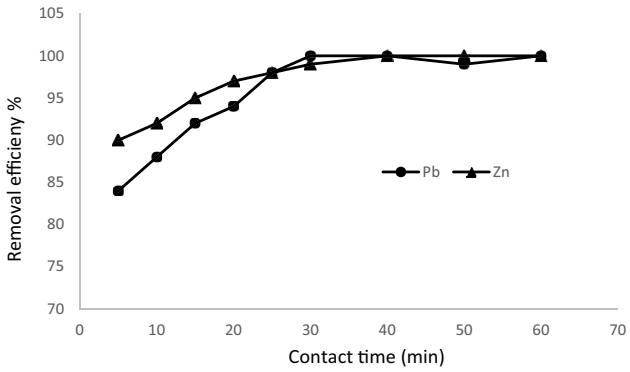

Fig. 8. Effect of contact time of the removal efficiencies of metal ions by GRN. In all of these experiments, 100 mg GRN was added to 50 mL solution with pH 4 containing 50 mg L^{-1} metal ion (Zn^{2+} or Pb^{2+}) and mixed for different times at room temperature.

Table 4
Pseudo-first-order kinetics and pseudo-second-order kinetics constants of lead and zinc ions sorption on GRN

Metal ion	C_0 (mg g^{-1})	First-order kinetics		Second-order kinetics	
		K_1 (min^{-1})	R^2	K_2 (g mg^{-1} min^{-1})	R^2
Pb(II)	50	0.2183	0.912	0.0736	0.9997
Zn(II)	50	0.1708	0.8333	0.0977	0.9999

In all of these experiments, 100 mg GRN was added to 50 mL solution with pH 4 containing metal ion with concentration of 50 mg L^{-1} and mixed for different times at room temperature.

adsorption but, this conclusion is not conclusive and should be proven by other experiments.

3.4.4. Adsorption studies

The initial concentration of the metal ion is an important parameter that can affect the removal efficiency. To evaluate this factor, some solutions with different concentrations of lead and zinc ions in the range of 50–150 mg L^{-1}. In practice, 4.0 mg mL^{-1} nanoparticles were added to each of solutions and stirred for 30 min. After centrifuging, the residual concentrations of lead and zinc ions were determined. Fig. 9 shows the results of these experiments. As it can be seen in Fig. 9, at initial concentration of 30 mg L^{-1} or lower, the ion removal is complete but, by increasing initial ion concentration, the removal efficiency is decreased due to the saturation of adsorption sites on GRN.

For clarification of adsorption mechanism, the adsorption data in Fig. 9 were checked by Langmuir, Freundlich, and Temkin isotherms. In the Langmuir model, there is a homogeneous surface of the sorbent, there is no interaction between the adsorbed species on adsorptive active sites, the adsorption is localized in a monolayer and it is assumed that once an ion occupies a site, no further adsorption can take place at that site.

Langmuir isotherm in linear form can be represented as Eq. (5) [43]:

$$\frac{C_e}{q_e} = \frac{1}{bq_m} + \frac{C_e}{q_m} \tag{5}$$

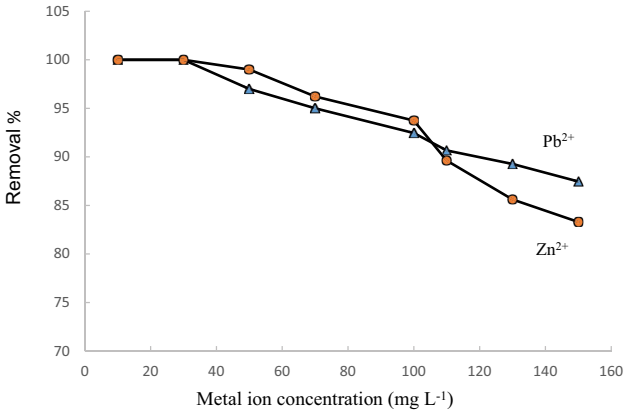

Fig. 9. Effects of initial concentration of lead and zinc ions on the removal efficiencies. All these experiments were done in conditions including 50 mL solution, contact time 30 min, pH 4, sorbent dosage 4 g L^{-1}, and temperature 25°C.

where C_e is the equilibrium concentration of Pb (II) in solution (mg L^{-1}), q_e is the equilibrium capacity (mg g^{-1}) of Pb (II), q_{max} is the maximum adsorption capacity of the sorbent corresponding to complete monolayer coverage on the surface (mg g^{-1}), and b is the Langmuir adsorption constant (L mg^{-1}) and related to the free energy of adsorption.

The linear form of Freundlich isotherm can be given as follows:

$$\log q_e = \log k_f + \frac{1}{n}\log C_e \tag{6}$$

where K_f is the constant related to the adsorption capacity of the sorbent in mg L^{-1}, and n is the constant related to the adsorption intensity.

The third isotherm is Temkin, which contains a factor that explicitly considers interactions between attraction and adsorption capacities [44,45] and can be identified as follows:

$$q_e = B\ln A + B\ln C_e \tag{7}$$

where A is the equivalent to the fixed Linked with maximum energy (L mg^{-1}), $B\left(B = \frac{RT}{b}\right)$ as a constant coefficient is proportional to the heat of adsorption, and b is the constant of Temkin isotherm (J mol^{-1}). The obtained results of three isotherms are shown in Fig. 10. As Fig. 10 shows the experimental data for the adsorption of lead and zinc ions on GRN are acceptably fitted with Langmuir isotherm. Langmuir isotherm compatibility can be another reason for chemical absorption. All examination of Fig. 10 was repeated by GRP. The summary of the calculated parameters of three isotherm models is presented in Table 5. The maximum adsorption capacities (q_{max}) based of the slope of Langmuir isotherm were found 24.6 and 26.3 mg g^{-1} for the adsorption of lead and zinc ions on GRN at 25°C, respectively. Based on the presented results in Table 5, GRN has greater adsorption capacity than GRP because the effective surface area of GRN is bigger.

For finding more reason for chemical adsorption, FT-IR spectrums were recorded before and after contacting GRN with lead and zinc ions (Fig. 11). In chemical adsorption of metal ions, it is expected that some bands of sorbent are shifted to blue or red shifts and one or more new bands is observed in wave numbers less than 1,000 cm^{-1} [46]. The score bands of FT-IR spectrums are summarized in Table 6.

As it is obvious in Table 6, there four functional groups (C=O: carbonyl, C–O: Ester, N–H: amine 1°, and N–H: amine 2°) on GRN which can interact with Pb and Zn ions. All of these

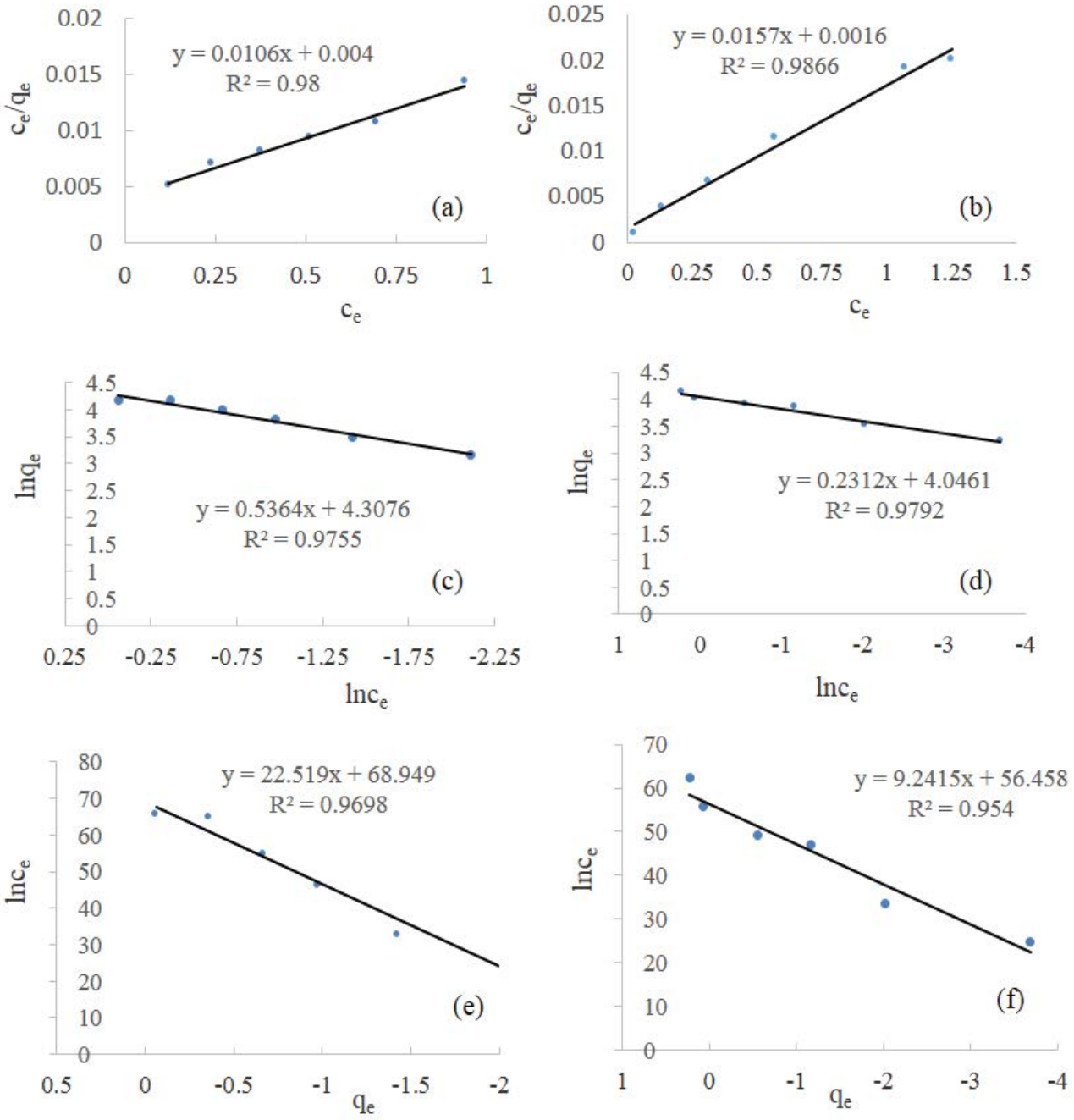

Fig. 10. Adsorption isotherms of metal ions on GRN; Langmuir isotherms for the adsorption of Pb^{2+} (a) and Zn^{2+} (b), Freundlich isotherms for the adsorption of Pb^{2+} (c) and Zn^{2+} (d) and Temkin isotherms for the adsorption of Pb^{2+} (e) and Zn^{2+} (f). In all of these experiments, 100 mg GRN was added to 50 mL solution with pH 4 containing metal ion (Zn^{2+} or Pb^{2+}) and mixed for 30 min at room temperature.

absorption bands are weakened and shifted to red wavelengths after interaction with metal ions. The Pb–O and Zn–O bands are formed and observed at 519.03 and 428.7 cm^{-1}, respectively. The findings of the FT-IR spectrums confirm the chemical absorption of metal ions on GRN.

3.4.5. Thermodynamic studies

The effect of solution temperature on the ion removal efficiency was studied (Fig. 12). The ion removal efficiencies decrease when the solution temperature increases. Therefore, it can be concluded that the adsorption of lead and zinc ions on GRN could be an exothermic process.

The mechanism of adsorption can identify its temperature dependency. The solution temperature has two major effects on the adsorption processes. The first effect is the direct dependency of diffusion rate of the adsorbate across the external boundary layer and in the internal pores of the sorbents. The second effect of the temperature is the variation of equilibrium capacity of the sorbent towards adsorbate

Table 5
Adsorption isotherm parameters of lead and zinc ions on GRN at 25°C

Isotherm model parameters		Pb^{2+}		Zn^{2+}	
		GRP	GRN	GRP	GRN
Langmuir	q_{max}	8.6	24.6	11.2	26.3
	k_1	136	250	335	625
	R^2	0.982	0.980	0.983	0.987
Freundlich	K_F	36.2	74.3	29.3	57.2
	N	1.8	1.9	3.7	4.3
	R^2	0.967	0.976	0.981	0.979
Temkin	A	20.654	21.387	398.601	449.702
	B	19.312	22.519	8.912	9.242
	R^2	0.970	0.970	0.960	0.954

[47–50]. To investigate the influence of temperature on the uptake of lead and zinc ions by the studied sorbent, the removal of these ions (50 mg L^{-1}) from aqueous solution at adjusted pH of 4 and GRN g L^{-1} was performed as a function of temperature in the range 283–343 K. The corresponding distribution coefficient (K_d) was calculated by Eq. (8):

$$K_d = \frac{(C_0 - C_e)}{C_e} \times \frac{V}{m} \tag{8}$$

where C_0 and C_e are initial and equilibrium concentrations of metal ions (mg L^{-1}), respectively, V is the volume of the aqueous sample solution (L), and m is the amount of sorbent (g). The Van't Hoff equation can be shown as Eq. (9):

$$\ln K_d = \frac{\Delta S}{R} - \frac{\Delta H^0}{RT} \tag{9}$$

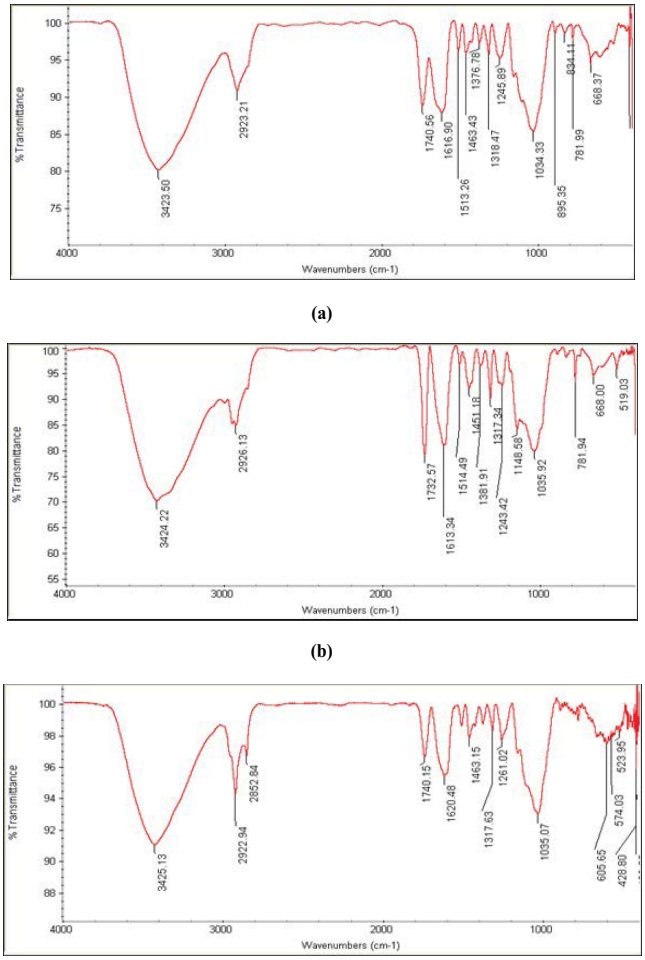

(a)

(b)

(c)

Fig. 11. FTIR spectrums GRN befor (a) and after (b) treating with lead ion solution, and after (c) treating with zinc ion solution.

Table 6
Absorption bands of FTIR spectrums of GRN before and after contact with Pb^{2+} and Zn^{2+} solutions

After interacting with the zinc ion	After interacting with the lead ion	Band	Before the interacting with the zinc and lead ions	No.
3,425.13	3,423.50	OH	3,424.22	1
2,922.29	2,923.21		2,926.13	2
1,740.50	1,740.56	Stretching of C=O (Carbonyl)	1,732.57	3
1,620.48	1,616.90	Bending of NH (Amin 1°)	1,613.34	4
–	1,513.26		1,514.49	5
1,463.15	1,463.43		1,451.18	6
–	1,376.78		1,381.91	7
1,317.63	1,318.47		1,317.34	8
1,226.02	1,245.89		1,243.42	9
–	1,034.33		1,148.58	10
–	–	Stretching of C–O (Ester)	1,035.95	11
–	834.11	Bending of NH (Amin 2°)	781.94	12
428.7	519.03	Stretching of MO (Pb–O or Zn–O)	–	13

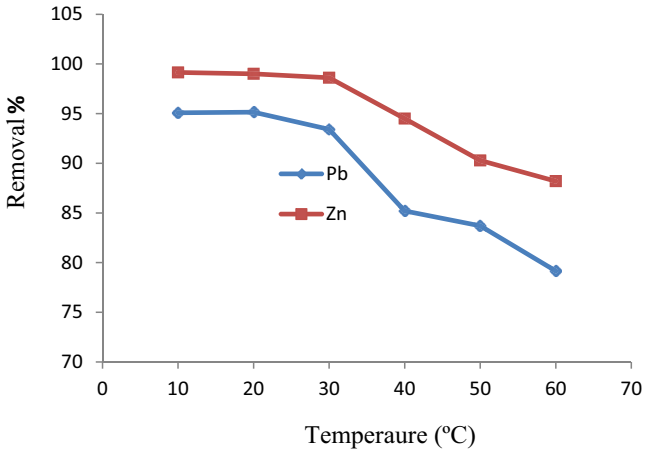

Fig. 12. Effect of temperature on the metal ion removal efficiency. The experimental conditions include solution volume 50 mL, contact time 30 min, pH 4, sorbent dosage 4 g L^{-1} and ion concentration 50 mg L^{-1}.

Based on Eq. (9), standard enthalpy ($\Delta H°$) and entropy ($\Delta S°$) changes can be analyzed by plotting the ln K_d versus T^{-1} [47]. The values of $\Delta H°$ and $\Delta S°$ were calculated from the slope and intercept of linear plot of ln K_d versus T^{-1}, respectively (Fig. 13).

Based on the presented plots in Fig. 13, $\Delta H°$ and $\Delta S°$ were calculated and then the Gibbs free energy changes ($\Delta G°$) determined by Eq. (10):

$$\Delta G^0 = \Delta H^0 - T\Delta S^0 \quad (10)$$

The calculated thermodynamic parameters for the adsorption process of lead and zinc ions on the sorbent are given in Table 7. The negative amount of $\Delta H°$ indicates that the adsorption of lead and zinc ion on GRN is an exothermic process. The negative amounts of $\Delta G°$ and $\Delta S°$ show that the adsorptions of both Pb^{2+} and Zn^{2+} on GRN are spontaneous processes and during adsorption, the entropy of the system is decreased, respectively [47,48].

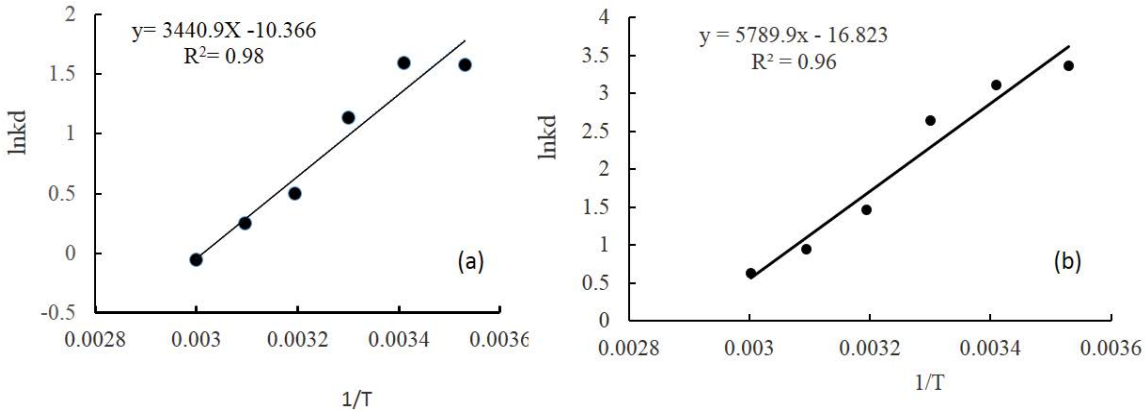

Fig. 13. Linear Van't Hoff plot of adsorption of Pb^{2+} (a) and Zn^{2+} (b) on GRN. In all of these experiments, 100 mg GRN was added to 50 mL solution with pH 4 containing metal ion (Zn^{2+} or Pb^{2+}) 50 mg L^{-1}.

Table 7
Summary of the calculated thermodynamic parameters for the adsorption of lead and zinc ions on GRN

Ion	$-\Delta H°$ (kJ mol^{-1})	$-\Delta S°$ (kJ $mol^{-1}K^{-1}$)	$-\Delta G°$ (kJ mol^{-1}) at temperatures (K)					
			283	293	303	313	323	333
Pb^{2+}	28.608	86.183	4.218	3.357	2.495	1.633	0.771	0.090
Zn^{2+}	48.137	139.866	8.555	7.156	5.758	4.359	2.960	1.561

Table 8
The features of the current nanobiosorbent have been compared with some previous works

No.	Ion	Sorbent	q_{max} (mg g^{-1})	pH	Temperature (°C)
[51]	Cd^{2+}	Cork	9.65	6	25
[16]	Pb^{2+}, Zn^{2+}	Cedar leaf	7.23, 4.79	5	20
[52]	Cu^{2+}, Pb^{2+}	Marula seed husk	10.2, 20	6, 5	20
[53]	Cu^{2+}	Banana peel	20.37	6.5	20
[54]	Cu^{2+}	Garden grass	58.34	6	20
Current work	Pb^{2+}, Zn^{2+}	GRP	8.6, 11.2	4	25
Current work	Pb^{2+}, Zn^{2+}	GRN	24.6, 26.3	4	25

3.4.6. Comparative features

In Table 8, some score parameters of the presented nano-biosorbent have been compared with some previous studies. As Table 8 shows GRN can remove Pb^{2+} and Zn^{2+} ions from water with more sorption capacities than those of Ref. [16] and about Pb^{2+} also more than [52].

4. Conclusions

The all particles prepared from roots of castor, pear, peach, apple, almond, walnut, sour cherry, berry, ginger, sunflower, red flower, mallow, grapevine, hot pepper, hollyhock, tomato, astragalus, and black eggplant plant roots can be used as biosorbents to remove some heavy metal ions from water. Among of them, pear, sour cherry, sunflower, mallow, grapevine, hot pepper, hollyhock, tomato, astragalus, and eggplant can be used as efficient biosorbents (removal efficiency more than 90%) for the removal of lead ions. The roots particles of grapevine and eggplant can be used as efficient biosorbents (removal efficiency more than 90%) for the removal of lead and zinc ions. The prepared GRN can quantitatively remove lead and zinc ions from water. Adsorption of Pb^{2+} and Zn^{2+} ions on GRN is described by Langmuir isotherm and pseudo-second-order kinetics model. Thermodynamic studies showed that the adsorptions of lead and zinc ions on GRN are spontaneous and exothermic processes. The prepared nanoparticles are inexpensive, available, abundant, healthy, and nontoxic, but it is a bit difficult to separate these nanoparticles from water due to their low density.

Acknowledgement

The authors would like to thank the financial support of this work by Abhar Payame Noor University Research Council.

References

[1] T.K. Naiya, A.K. Bhattacharya, S.K. Das, Adsorption of Cd(II) and Pb(II) from aqueous solutions on activated alumina, J. Colloid Interface Sci., 333 (2009) 14–26.
[2] A.R. Ngomsik, A. Bee, J.M. Siaugue, D. Talbot, V. Cabuil, G. Cote, Co (II) removal by magnetic alginate beads containing Cyanex, J. Hazard. Mater., 166 (2009) 1043–1049.
[3] B. Acemioglu, M.H. Alma, Equilibrium, adsorption of Cu(II) from aqueous solution onto cellulose, J. Colloid Interface Sci., 243 (2001) 81–84.
[4] T. Depci, A.R. Kul, Y. Onal, Competitive adsorption of lead and zinc from aqueous Solution of activated carbon prepared from the Van apple pulp: study in single-and multi solute systems, J. Chem. Eng., 200–202 (2012) 224–236.
[5] J.M. Barbosa, C. Lopez-Velandia, A. Maldonado, L. Giraldo, J. Moreno-Pirajan, Removal of lead(II) and zinc(II) ions from aqueous solutions by adsorption onto activated carbon synthesized from watermelon shell and walnut shell, Adsorption, 19 (2013) 675–685.
[6] D. Ozdes, A. Gundogdu, B. Kemer, C. Duran, H.B. Senturk, M. Soylak, Removal of Pb(II) ions from aqueous solution by a waste mud from copper mine industry: equilibrium, kinetic and thermodynamic study, J. Hazard. Mater., 166 (2009) 1480–1487.
[7] M.D. Meitei, M.N.V. Prasad, Adsorption of Cu (II), Mn (II) and Zn (II) by *Spirodela polyrhiza* (L.) Schleiden: equilibrium, kinetic and thermodynamic studies, J. Ecol. Eng., 71 (2014) 308–317.
[8] T.A. Kurniawan, G.Y. Chan, W.-H. Lo, S. Babel, Physico–chemical treatment techniques for wastewater laden with heavy metals, Chem. Eng. J., 118 (2006) 83–98.
[9] Y.H. Wang, S.H. Lin, R.S. Juang, Removal of heavy metal ions from aqueous solutions using various low-cost adsorbents, J. Hazard. Mater., 102 (2003) 291–302.
[10] J.F. Blais, S. Shen, N. Meunier, R.D. Tyagi, Comparison of natural adsorbents for metal removal from acidic effluent, Environ. Technol., 24 (2003) 205–215.
[11] A. Bhatnagar, V.J.P. Vilar, J.C. Santos, C.M.S. Botelho, R.A.R. Boaventura, Valorisation of marine *Pelvetia canaliculata* Ochrophyta for separation and recovery of nickel from water: equilibrium and kinetics modeling on Na-loaded algae, Chem. Eng. J., 200 (2012) 365–372.
[12] H.K. Boparai, M. Joseph, D.M. Ocarroll, Kinetics and thermodynamics of cadmium ion removal by adsorption onto nano zero-valent iron particles, J. Hazard. Mater., 186 (2011) 458–465.
[13] X. Xin, Q. Wei, J. Yang, L. Yan, R. Feng, G. Chen, B. Du, H. Li, Highly efficient removal of heavy metal ions by amine-functionalized mesoporous Fe_3O_4 nanoparticles, Chem. Eng. J., 184 (2012) 132–140.
[14] A. Rahmani, H.Z. Mousavi, M. Fazli, Effect of nanostructure alumina on adsorption of heavy metals, Desalination, 253 (2010) 94–100.
[15] K.K. Wong, C.K. Lee, K.S. Low, Removal of Cu and Pb by tartaric acid modified rice husk from aqueous solution, Chemosphere, 50 (2003) 23–28.
[16] L.D. Hafshejani, S.B. Nasab, R.M. Gholami, M. Moradzadeh, Z. Izadpanah, S.B. Hafshejani, A. Bhatnagar, Removal of zinc and lead from aqueous solution by nanostructured cedar leaf ash as biosorbent, J. Mol. Liq., 211 (2015) 448–456.
[17] E. pehlivan, T. Altun, S. parlayici, Modified barley straw as a potential biosorbent for removal of copper ions from aqueous solution, Food Chem., 135 (2012) 2229–2234.
[18] M. Moyo, U. Guyo, G. Mawenyiyo, N. Zinyama, B. Nyamunda, Marula seed husk biomass as a low cost biosorbent for removal of Pb(II) and Cu(II) from aqueous solution, J. Ind. Eng. Chem., 27 (2015) 126–132.
[19] S. Thakur, S. Kumari, P. Dogra, G. Chauhan, A new guar gum-based adsorbent for the removal of Hg(II) from its aqueous solutions, Carbohydr. Polym., 106 (2014) 276–282.
[20] H. Karami, A. Sadeghi, S.R. Mirghasemi, Iranian Paptent No. 62129, 2009.
[21] M. Ahmaruzzaman, V.K. Gupta, Rice husk and its ash as low cost adsorbents in water and wastewater treatment, Ind. Eng. Chem. Res., 50 (2011) 13589–13613.
[22] Z. Aksu, Application of biosorption for the removal of organic pollutants: a review, Process Biochem., 40 (2005) 997–1026.
[23] I. Ali, V.K. Gupta, Advances in water treatment by adsorption technology, Nat. Protoc., 1 (2006) 2661–2667.
[24] S.E. Bailey, T.J. Olin, R.M. Bricka, D.D. Adrian, A review of potentially low-cost sorbents for heavy metals, Water Res., 33 (1999) 2469–2479.
[25] N. Das, Remediation of radionuclide pollutants through biosorption: an overview, Clean Soil Air Water, 40 (2012) 16–23.
[26] A. Demirbas, Heavy metal adsorption onto agro-based waste materials: a review, J. Hazard. Mater., 157 (2008) 220–229.
[27] G.M. Gadd, Biosorption: critical review of scientific rationale, environmental importance and significance for pollution treatment, J. Chem. Technol. Biotechnol., 84 (2009) 13–28.
[28] V.K. Gupta, P.J.M. Carrott, M.M.L. Ribeiro Carrott, Low cost adsorbents: growing approach to wastewater treatment: a review, Crit. Rev. Environ. Sci. Technol., 39 (2009) 783–842.
[29] A. Kapoor, T. Viraraghavan, Fungal biosorption an alternative treatment option for heavy metal bearing wastewaters: a review, Bioresour. Technol., 53 (1995) 195–206.
[30] E. Romera, F. Gonzalez, A. Ballester, M.L. Blazquez, J.A. Munoz, Biosorption with algae: a statistical review, Critl. Rev. Biotechnol., 26 (2006) 223–235.
[31] D. Sud, G. Mahajan, M.P. Kaur, Agricultural waste material as potential adsorbent for sequestering heavy metal ions from aqueous solutions: a review, Bioresour. Technol., 99 (2008) 6017–6027.
[32] F. Veglio, F. Beolchini, Removal of metals by biosorption: a review, Hydrometallurgy, 44 (1997) 301–316.

[33] K. Vijayaraghavan, Y.S. Yun, Bacterial biosorbents and biosorption, Biotechnol. Adv., 26 (2008) 266–291.
[34] W.T. Tan, S.T. Ooi, C.K. Lee, Removal of chromium (VI) from solution by coconut husk and palm pressed fibers, Environ. Technol., 14 (1993) 277–282.
[35] H. Parab, S. Joshi, N. Shenoy, A. Lali, U.S. Sarma, M. Sudersanan, Determination of kinetic and equilibrium parameters of the batch adsorption of Co(II), Cr(III) and Ni(II) onto coir pith, Process Biochem., 41 (2006) 609–615.
[36] H. Parab, S. Joshi, N. Shenoy, R. Verma, A. Lali, M. Sudersanan, Uranium removal from aqueous solution by coir pith: equilibrium and kinetic studies, Bioresour. Technol., 96 (2005) 1241–1248.
[37] H. Parab, M. Sudersanan, Engineering a lignocellulosic biosorbent–coir pith for removal of cesium from aqueous solutions: equilibrium and kinetic studies, Water Res., 44 (2010) 854–860.
[38] H. Parab, N. Shenoy, S.A. Kumar, S.D. Kumar, A.V.R. Reddy, Removal of strontium from aqueous solutions using coir pith as biosorbent: kinetic and equilibrium studies, Int. J. Curr. Res., 5 (2013) 3697–3704.
[39] M. Yunus pamukoglu, F. Kargi, Removal of copper (II) ions from aqueous medium by biosorption onto powdered waste sludge, Process Biochem., 41 (2006) 1047–1054.
[40] A. Gala, S. Sanak-Rydlewska, A comparison of Pb^{2+} sorption from aqueous solutions on walnut shells and plum stones, Pol. J. Environ. Stud., 20 (2011) 877–883.
[41] Y. Ho, Review of second-order models for adsorption systems, J. Hazard. Mater., 136 (2006) 681–689.
[42] B. Cheng, Y. Le, W. Cai, J. Yu, Synthesis of hierarchical $Ni(OH)_2$ and NiO Nano sheets and their adsorption kinetics and isotherms to Congo red in water, J. Hazard. Mater., 185 (2011) 889–897.
[43] S. Liang, X. Guo, N. Feng, Q. Tian, Adsorption of Cu^{2+} and Cd^{2+} from aqueous solution by mercator-acetic acid modified orange peel, Colloids Surf. B, 73 (2009) 10–14.
[44] M. Ozacar, I.A. Şengil, Adsorption of metal complex dyes from aqueous solutions by pine sawdust, Bioresour. Technol., 96 (2005) 791–795.
[45] I.D. Mall, V.C. Srivastava, N.K. Agarwall, I.M. Mishra, Removal of congo red from aqueous solution by bagasse fly ash and activated carbon: kinetic study and equilibrium isotherm analyses, Chemosphere, 61 (2005) 492–501.
[46] R. Wang, Q. Li, D. Xie, H. Xiao, H. Lu, Synthesis of NiO using pine as template and adsorption performance for Pb(II) from aqueous solution, Appl. Surf. Sci., 279 (2013) 129–136.
[47] P. Sharma, R. Tomar, Synthesis and application of an analogue of mesolite for the removal of uranium(VI), thorium(IV), and europium(III) from aqueous waste, Micropor. Mesopor. Mater., 116 (2008) 641–652.
[48] S. Wang, Y. Boyjoo, A. Choueib, Z.H. Zhu, Removal of dyes from aqueous solution using fly ash and red mud, Water. Res., 39 (2005) 129–138.
[49] B. Song, G. Zeng, J. Gong, P. Zhang, M. Cheng, Effect of multi-walled carbon nanotubes on phytotoxicity of sediments contaminated by phenanthrene and cadmium, Chemosphere, 172 (2017) 449–458.
[50] B. Song, P. Xu, G. Zeng, J. Gong, S. Ye, Modeling the transport of sodium dodecyl benzene sulfonate in riverine sediment in the presence of multi-walled carbon nanotubes, Water Res., 129 (2018) 20–28.
[51] F. Krika, N. Azzouz, M. Chaker Ncibi, Adsorptive removal of cadmium from aqueous solution by cork biomass, Arabian J. Chem., 9 (2016) 1077–S1083.
[52] M. Moyo, U. Guyo, G. Mawenyiyo, N.P. Zinyama, B.C. Nyamunda, Marula seed husk (*Sclerocarya birrea*) biomass as a low cost biosorbent for removal of Pb(II) and Cu(II) from aqueous solution, J. Ind. Eng. Chem., 27 (2015) 126–132.
[53] M.A. Hossain, H.H. Ngo, W.S. Guo, T.V. Nguyen, Biosorption of Cu(II) from water by banana peel based, J. Water Sustain., 2 (2012) 87–104.
[54] M.A. Hossain, H.H. Ngo, W.S. Guo, T. Setiadi, Adsorption and desorption of copper (II), Bioresour. Technol., 121 (2012) 386–395.